Support Information

Rational Designed Water-soluble AIE Fluorescent Polyester for the Detection of Oligomers Based on the Characteristics of HEWL Amyloid Fibrosis

Zhimin Lu,[a] Yixiu Wang,[b] Junyong Zhang,[a] Anrong Mao*[b] and Meidong Lang*[a]

[a] Key Laboratory for Ultrafine Materials of Ministry of Education, School of Materials Science and Engineering, East China University of Science and Technology, Shanghai 200237, China.

[b] Department of Hepatic Surgery, Fudan University Shanghai Cancer Center, Department of Oncology, Shanghai Medical College, Fudan University, Shanghai 200032, China.

Table of contents

1. Experimental

1.1 Materials

Poly (ethylene glycol) methylether ($mPEG_3$) and stannous isooctanoate ($Sn(Oct)_2$) were purchased from Sigma-Aldrich. HEWL was purchased from Psaitong. Other solvents and chemicals were obtained from Adamas. Solvents used in reactions were dried over CaH_2 or anhydrous magnesium sulfate and stored under inert-gas protection.

1.2 Characterization

^1H and ^{13}C NMR spectra of polymer were recorded by Bruker AV apparatus at frequencies of 400 MHz and 100 MHz, with D_2O, Chloroform-d, or DMSO-d_6 as solvents. The number-average molecular weight (M_n) and dispersity (Đ) values were measured via gel permeation chromatography (GPC), DMF as the mobile phase at a flow rate of 1 mL/min. The GPC column was TSK gel Alpha column, with the temperature of 50 °C, using narrow-distribution PMMA as the standard. FT-IR spectra at frequencies ranging from 400 to 4000 cm^{-1} were recorded by Thermo Scientific Nicolet 5700 IR spectrometer. The fluorescence spectrum of polymers and samples were recorded by LS-55 Lumine/Fluorescence spectrometer. Zetasizer 3000HS apparatus was used to measure the Zeta potential of samples. A JEM-1400 (Japan) transmission electron microscope (TEM) was used. Protein aggregates were visualized using the Nikon A1R confocal laser scanning microscope with a 100x lens and a 405 nm laser. Ultraviolet-visible light absorption spectroscopy is used to analyze the changes in the absorbance of ultraviolet light and visible light of samples.

1.3 Synthesis of Functionalized Tetraphenylethylene and Lactone Monomers

The tetrastyrene derivative (4-(1,2,2-triphenylvinyl) aniline, TPE-NH_2) was prepared by McMurry coupling reaction. Under argon protection, 6.00 g of active zinc powder and 250 mL of tetrahydrofuran were added to a 500 mL round-bottom flask. The flask was placed in a low temperature reactor and cooled to -10 °C, and titanium tetrachloride ($TiCl_4$) was slowly added to the 500 mL flask by means of a constant pressure dropping funnel. After the dropwise addition of $TiCl_4$ was complete, the reaction was warmed to room temperature and then refluxed in an oil bath at 60°C for 2.5 hours. After refluxing, a brown-black reaction solution was obtained, and 4.37 g (24 mmol) of benzophenone and 3.94 g (20 mmol) of 4-amino benzophenone were added, and the reflux was continued for 20 hours. The end point of the reaction was judged by thin layer chromatography. After the reaction was completed, the reaction was quenched with 10% potassium carbonate aqueous solution, the product was extracted with dichloromethane (DCM) (250 mL, 3 times), the filtrate was concentrated, and purified by petroleum column chromatography to separate ether-dichloromethane (1:10) The product 4-(1,2,2-triphenylvinyl) aniline (TPE-NH_2) was obtained as a

yellow powder. The product is prone to oxidative deterioration and needs to be stored in an inert atmosphere.

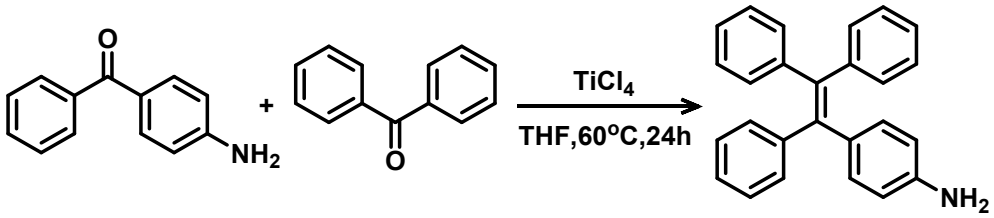

Fig. S1. Synthetic route of 4-(1,2,2-triphenylvinyl) aniline (TPE-NH_2).

The synthesis of 6-methylbenzyl acetate-ε-caprolactone 6-(CH_3)BCL monomer refers to the previous work[1, 2] of our group. As shown in Fig. S2, with cyclohexanone as the reaction raw material, functionalized caprolactone is prepared through Michael, hydrolysis, substitution and oxidation reactions. The synthesized functionalized monomer is a mixture of 2 substitution and 6 substitution. The substitution products of the two are isomers of each other. This is mainly due to the selective. production of nucleophilic substitution during the Baeyer-Villiger oxidation reaction.

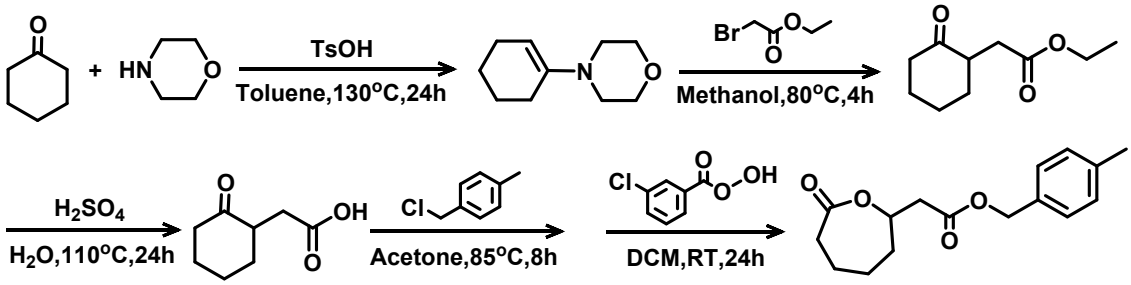

Fig. S2. Synthetic route of functional monomer 2(6)-methylbenzyl acetate-ε-caprolactone (BCL).

The synthesis of tert-butyl 7-oxo-1,4-oxazepane-4-carboxylate monomer, as shown in Fig. S3, with tert-butyl 4-oxopiperidine-1-carboxylate as the reaction raw material, functionalized caprolactone is prepared by Baeyer-Villiger oxidation reaction.

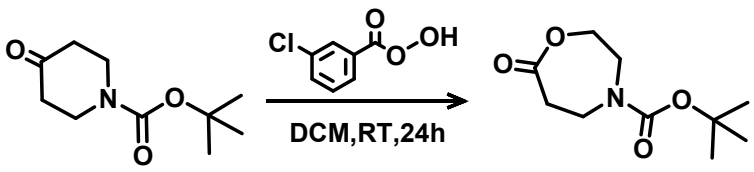

Fig. S3. Synthetic route of functional monomer 4-N-tert-Isobutylcarboxylate-piperolactone derivative (NIPIL).

1.4 Preparation of HEWL amyloid fibrils

The preparation process of HEWL amyloid fibrils refers to the reported method.[3] HEWL (Lyophilized, 200 mg) purchased from Psaitang, was added to 20 mL of CH_3COONa/CH_3COOH buffer solution (10 mmol/L, pH = 3) containing NaCl (100 mmol/L), and the solution concentration was 10 mg/mL (700 μmol/L). The samples were incubated at 70 °C at a stirring speed of 250 rpm. Samples were taken at regular intervals and stored in a refrigerator at 4 °C. After incubation for 1 hour, with the production of HEWL amyloid fibers, the clear solution turned into milky white turbid liquid. In order to ensure the accuracy of the experiment, the sampling time and experimental time shall not exceed 24 hours.

1.5 Confirmation of the process of amyloid fibrosis

The fluorescence characteristic curve of HEWL was measured with ThT and ANS to judge the degree of protein fibrosis and products of each stage. The changes of absorbance and transmittance were measured by UV-Vis spectrophotometer. The change of surface Zeta potential was measured by dynamic light scattering (DLS), and the morphology of HEWL was observed by TEM.

1.6 Synthesis of mPEG-(NIPIL-*co*-BCL)

Take $mPEG_3$-($NIPIL_{40}$-*co*-BCL_{10}) as an example. The 10 mL reaction eggplant bottle was fully dried, and NIPIL (0.8600 g, 4.0 mmol) and BCL (0.2760 g, 1.0 mmol) were added under the protection of argon. Using $mPEG_3$ (0.0163 g, 0.1 mmol) as the initiator and $Sn(Oct)_2$ as the catalyst (the dosage is 5% of the monomer mass), the ring-opening copolymerization was carried out at 130 °C. After 5 hours, the reaction was cooled and repeatedly precipitated with ether, dried and stored.

1.7 Fluorescence modification of mPEG-(PIL-*co*-CCL)-*g*-TPE

Take $mPEG_3$-(PIL_{40}-*co*-CCL_{10})-*g*-TPE as an example. Dissolved the product from the previous step in DCM, and added 2.0 mL HBr/CF_3COOH for 0.5 hour. After the reaction, precipitation was repeated with ether. The product was collected and dissolved in DCM, then EDC/NHS was added (the dosage is 1.5 times the molar amount of the amino group). After the solution became turbid, the amino functionalized tetraphenyl group (TPE-NH_2, 0.3470 g, 0.1 mmol) was added. After 24 hours of reaction, the target product was obtained by precipitation with a large amount of ethanol for several times.

1.8 pH responsiveness of polymer

A series of pH buffer solutions were prepared with pH values ranging from 3.8 to 9.18. And it was used to dissolve the polymer, and it was fully shaken to finally obtain a polymer solution with

a concentration of 0.2 mg/mL. The fluorescence intensity and Zeta potential of each group of samples were recorded.

1.9 Fluorescence detection for oligmers

Taking 0.2 mL (100 mg/mL) HEWL with different incubation times, added 3.5 mL of buffer solution with different pH value (pH=4.0 or 7.18), and then added 0.3 mL (1 mg/mL) of polymer aqueous solution. After fully shaking, the fluorescence spectra and CLSM images of the samples were recorded.

1.10 Preparation of THT and ANS solution

ThT: adding 0.0032 g THT to 10 mL phosphate buffer solution (pH=7.4, 20 mM) to get 10 mM ThT solution. When using, take 10 μL sample (concentration is 20 mg/mL), add a certain amount of Tris-HCl solution (10 mM, pH=8), and then added 30 μL THT solution, so that the final concentration of THT is 10 μM. The detection conditions are as follows: excitation light wavelength 440 nm, scanning the fluorescence spectrum of 450-550 nm.

ANS: adding 0.0299 g ANS to 10 mL double distilled water, the concentration of 10 mM ANS solution was obtained. When in use, a certain amount of samples to be tested were added to the working solution of ANS, so that the concentration ratio of ANS to protein is 17:1. The detection conditions are as follows: excitation light wavelength 370 nm, scanning the fluorescence spectrum of 400-600 nm.

2. Results And Discussion

2.1 Characterization of the product

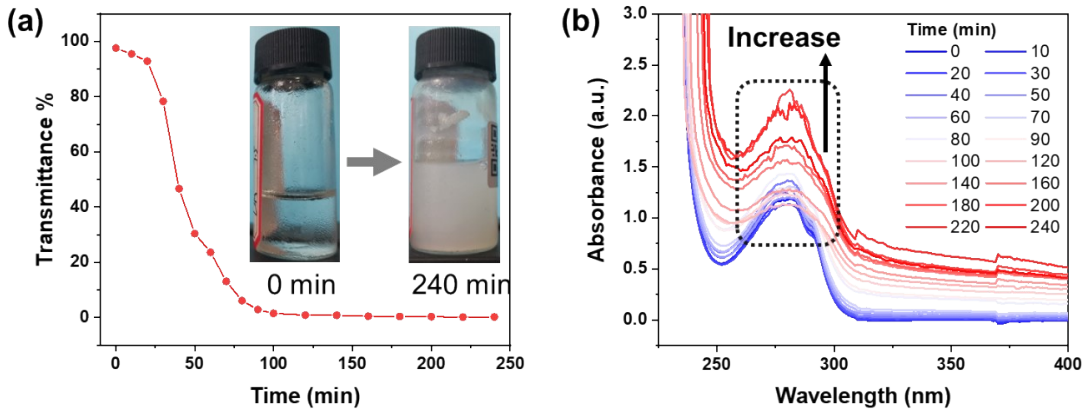

Fig. S4. (a) HEWL after incubation for different times (a) Changes in transmittance at 500 nm (the inset is a photo of the sample at 0 and 240 min); (b) Changes in UV-Vis absorption intensity

Discussion: The change of light transmittance of HEWL measured by UV-Vis spectrophotometer. As shown in Fig. S3a, the light transmittance of the HEWL solution did not change much from 0 to 20 min. Within 20-90 min, the light transmittance decreased rapidly, and the solution changed from colorless and transparent to white turbid. After 90 min, the solution was still white cloudy liquid with no obvious change. This phenomenon indicated that the water solubility and aggregation degree of HEWL were changed. The change in UV absorption intensity was further measured (Fig. S3b). It was found that the UV absorption at 280 nm increased significantly with the prolongation of incubation time, showing typical hyperchromic effect. In general, this enhanced UV absorption is mainly due to the increased surface content of three aromatic amino acids in proteins, including tyrosine, tryptophan, and phenylalanine. This indicates that during amyloid fibrosis, the higher-order structure of the protein is destroyed and the hydrophobic groups inside the molecule are exposed.

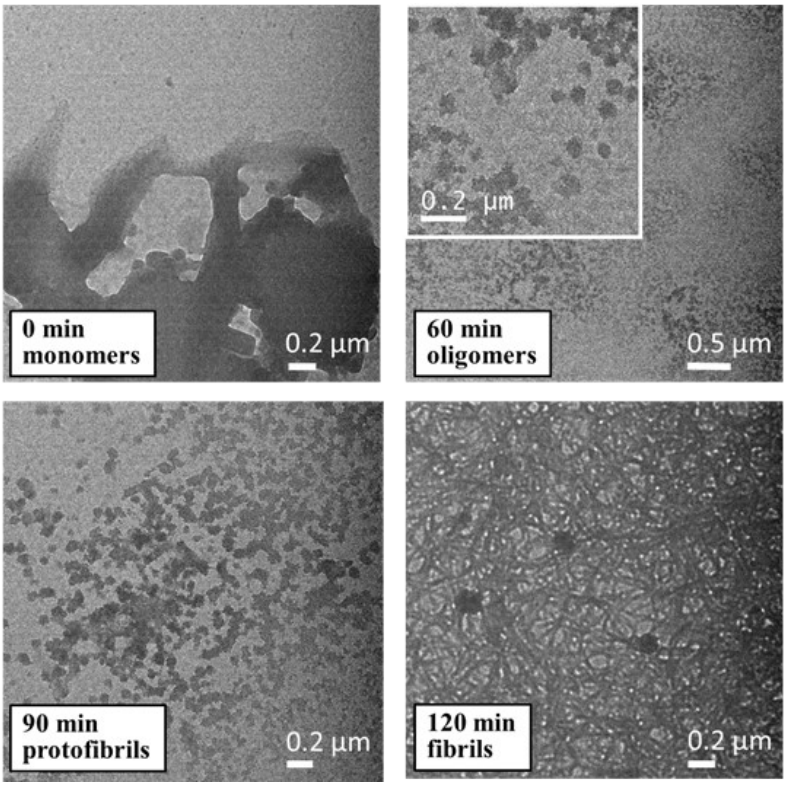

Fig. S5. (a) TEM images of HEWL incubated for different times

Discussion: TEM was used to observe the morphological changes of HEWL in the process of amyloid

fibrosis. As shown in Fig. 1c, it was found that the unincubated HEWL (0 min) has gradient protein membranes at the edges of aggregates. After incubation for 60 min, HEWL is granular and the particle size less than 100 nm. After incubation for 90 min, short fibers began to form, and some of them are longer than 0.2 μm. After 120 min of incubation, it was found that the protein morphology had been completely transformed into fibers, and the network structure composed of fibers was shown due to the concentration. And it may be that the fiber is wound during stirring, resulting in the formation of a small amount of spherical aggregates. The three main forms of protein aggregation in the process of fibrosis were directly proved by TEM, namely, globular (oligomers), short fiber (protofibers) and long fiber (mature fibers).

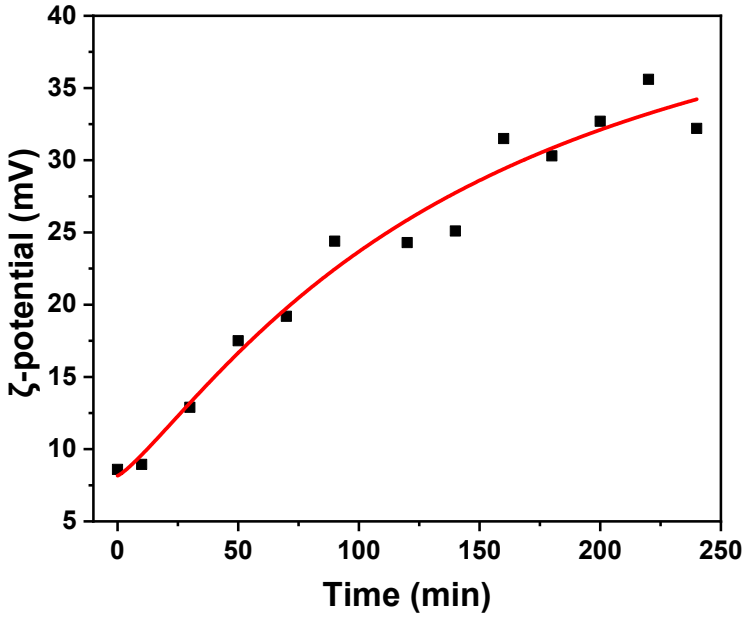

Fig. S6. Zeta potential of HEWL incubated for different times

Discussion: To further characterize the fibrosis process, the surface charge of the protein was measured. It can be found that in the process of fibrosis, the Zeta potential of HEWL increases continuously in the range of 0-240 min. specifically, within 0-80 min, the Zeta potential increased rapidly, indicating that the positive charge increased; within 80-240 min, the growth rate of Zeta potential slowed down. This indicates that during protein fibrosis, the aggregate charge also changes with the adjustment of surface chemical groups. Therefore, the change of charge may also be one of the important features during HEWL fibrosis.

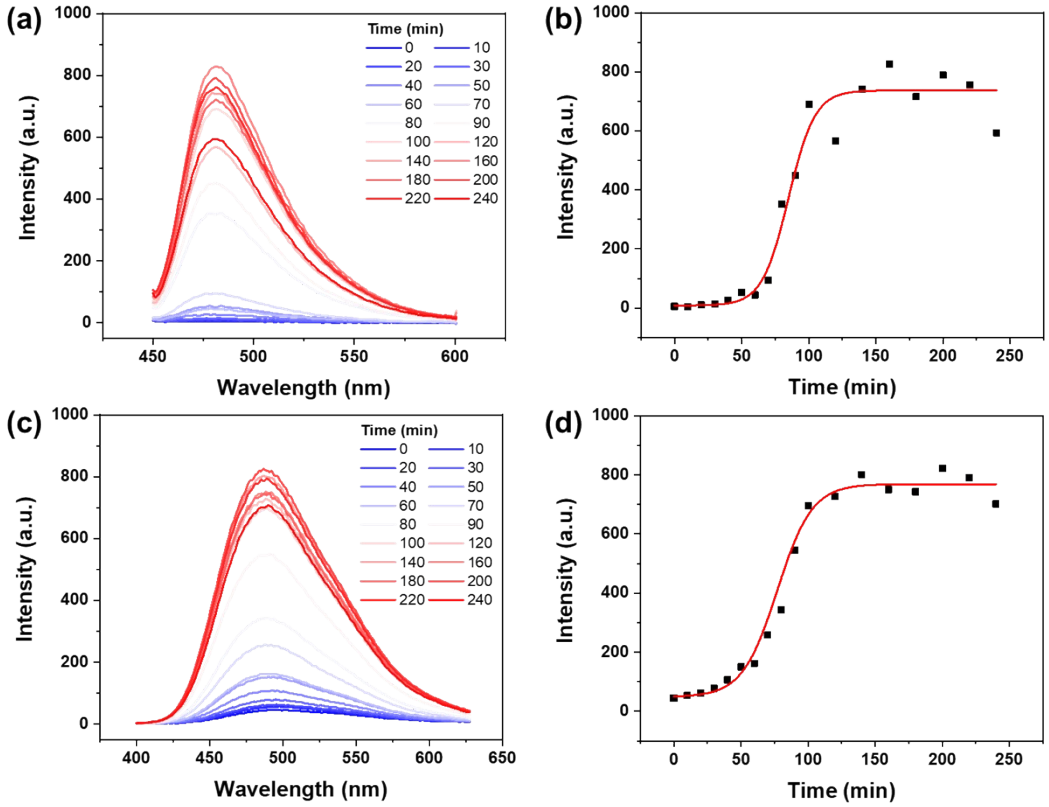

Fig. S7. HEWL after incubation for different times, (a) ThT and (c) ANS characteristic fluorescence emission spectrum; The intensity change of the maximum emission peak of (b) ThT and (c) ANS.

Discussion: ThT and ANS are commercial dyes for detecting amyloid fibrils due to their characteristics of binding to the β-sheet and hydrophobic structures in amyloid fibrils, respectively. ThT and ANS characteristic fluorescence spectra of amyloid fibrils at different incubation times were determined. The ThT fluorescence intensity of HWEL was found to be basically unchanged during 0-60 min of incubation, indicating that the secondary structure of HEWL changed slowly and was in the process of nucleation. During 60-120 min, the fluorescence signal increased rapidly, indicating a rapid increase of β-sheet. after 120 min, although the fluorescence intensity fluctuated to some extent, it remained stable with high emission intensity, indicating that the fibrillation process was basically completed and the HEWL structure was in a mature fibrillation state. In addition, ANS was used to reflect the degree of exposure of hydrophobic groups of the protein. The results showed that HEWL was in an enhanced state during 0-60 min of incubation, but the growth rate was not fast, indicating that the exposure of hydrophobic groups of proteins increased slowly. In 60-120 min, the fluorescence signal increased rapidly, and the surface hydrophobic groups increased rapidly. after 120 min, the fluorescence intensity fluctuated to

some extent, but remained in a stable state and the emission intensity was relatively high. Both curves also fit the sigmoidal curve.

The results indicate that the protein HEWL can be transformed into amyloid fibrils in a certain period of time when cultured under acidic and high temperature conditions. During the transition of amyloid fibrosis, the secondary structure of the β-sheet increases and the hydrophobic regions within the protein are exposed. These two structural changes occur simultaneously. The three stages can be roughly divided into 0-60 min, 60-120 min and 120 min later. And the corresponding products are roughly oligomers, protofibers and mature fibrils.

2.2 Characterization of the materials

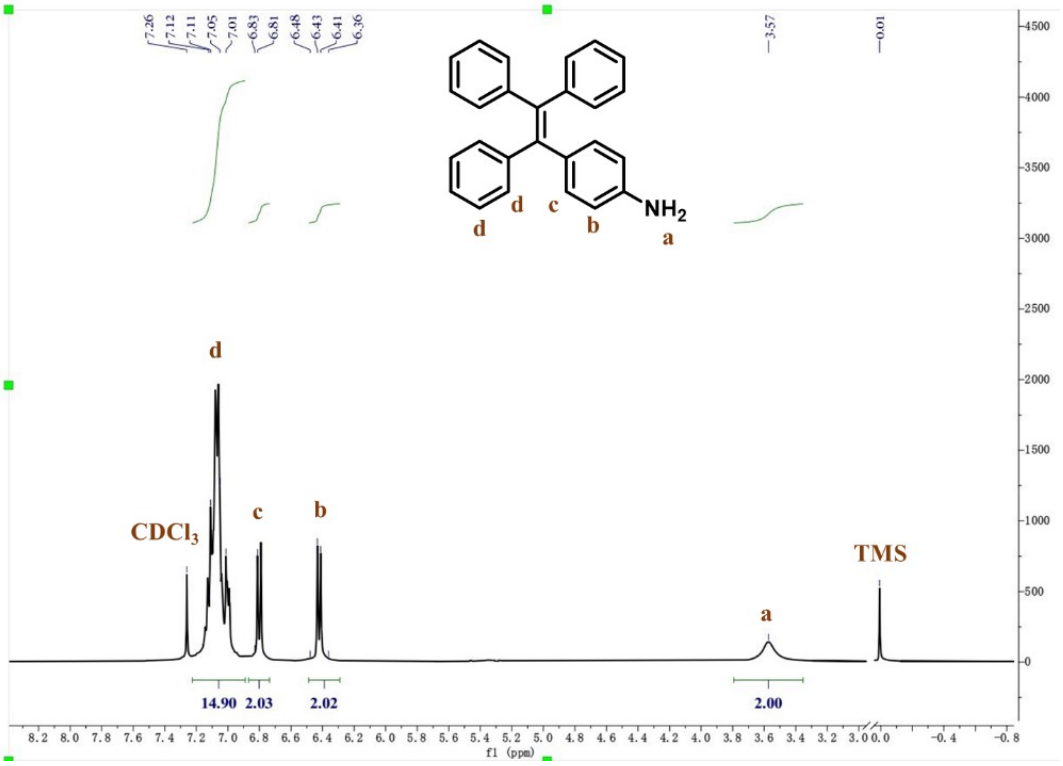

Fig. S8. ^{1}H NMR spectrum of amino-modified tetraphenylethylene (TPE-NH_2).

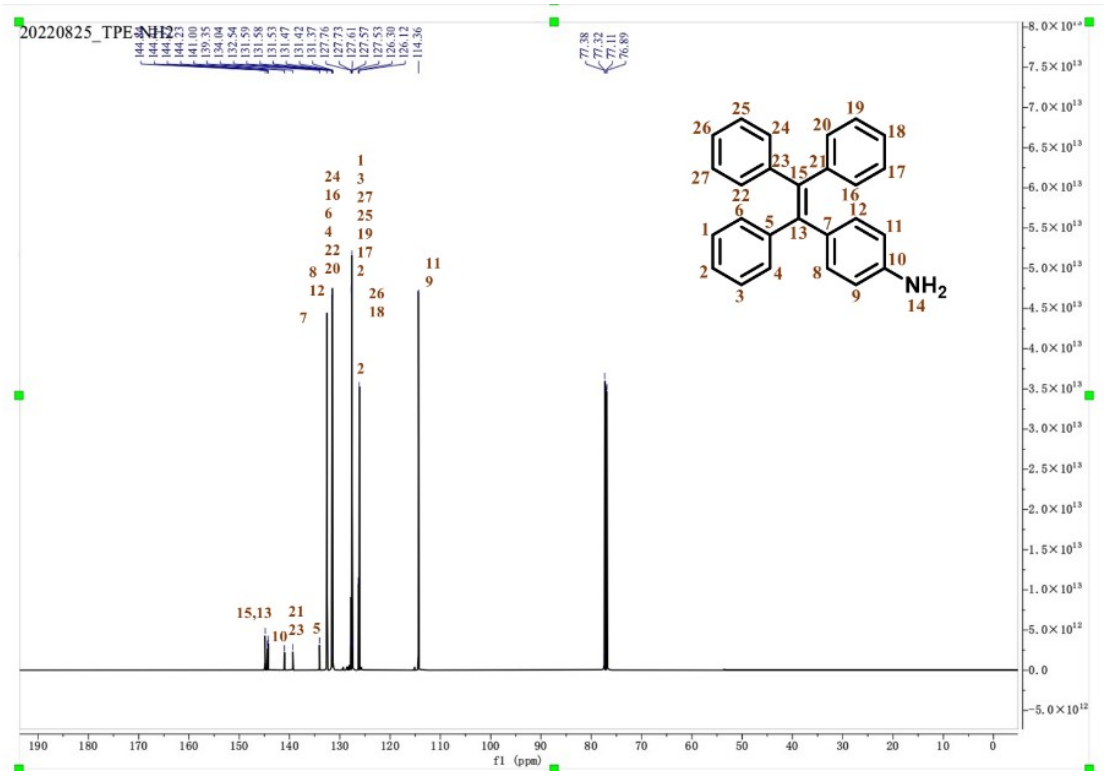

Fig. S9. ^{13}C NMR spectrum of amino-modified tetraphenylethylene (TPE-NH_2).

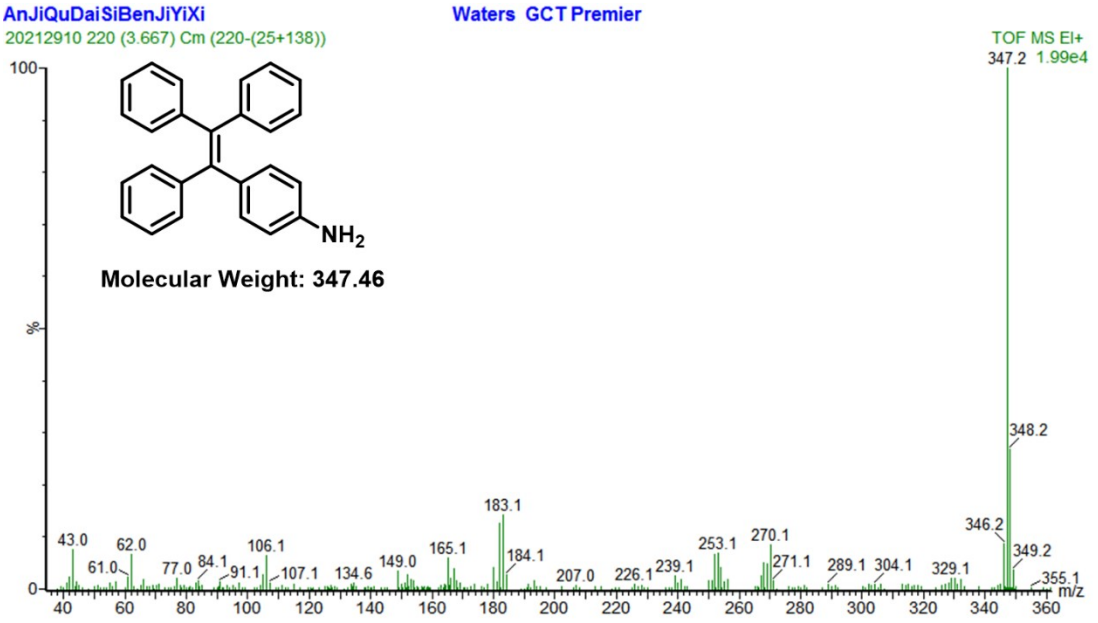

Fig. S10. Electron impact high resolution time-of-flight mass spectrometer of TPE-NH_2.

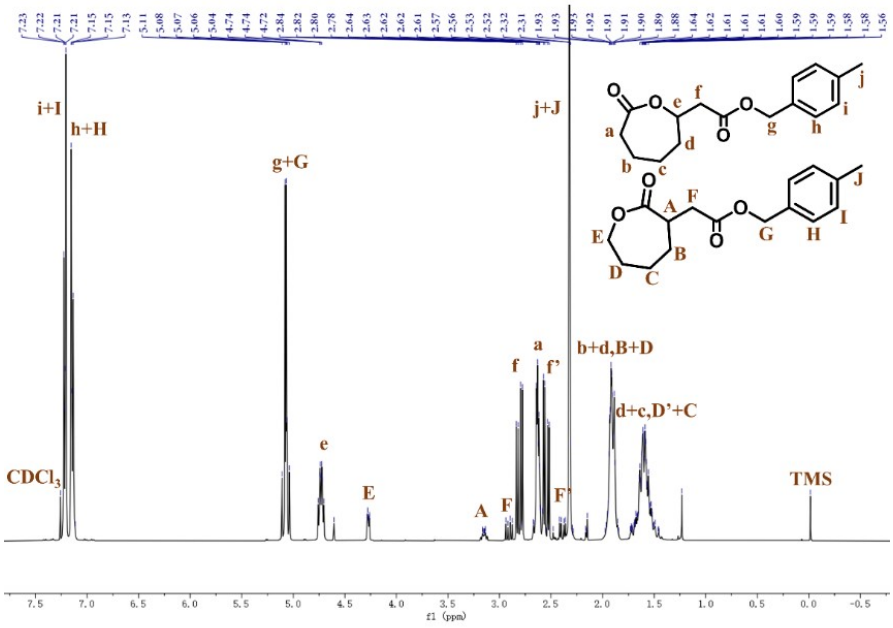

Fig. S11. ^{1}H NMR spectrum of 2(6)-CH_3-BCL.

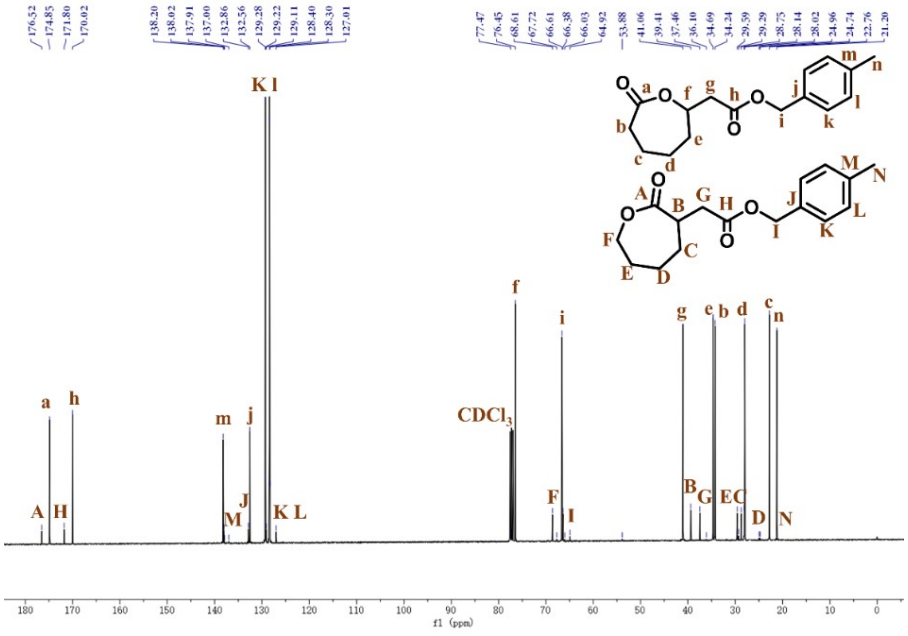

Fig. S12. ^{13}C NMR spectrum of 2(6)-CH_3-BCL.

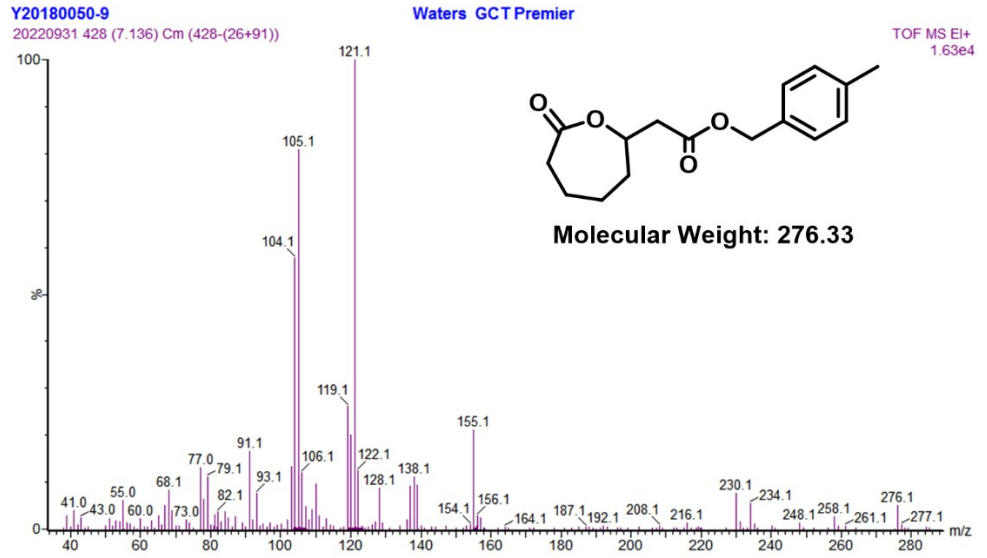

Fig. S13. Electron impact high resolution time-of-flight mass spectrometer of 2(6)-CH_3-BCL

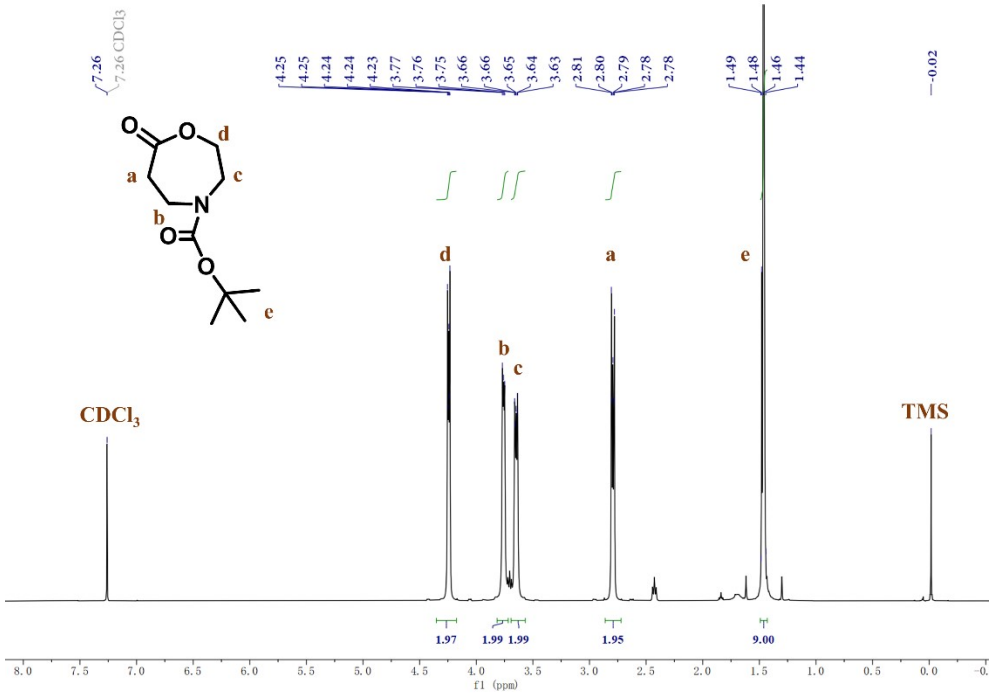

Fig. S14. ^{1}H NMR spectrum of NIPIL

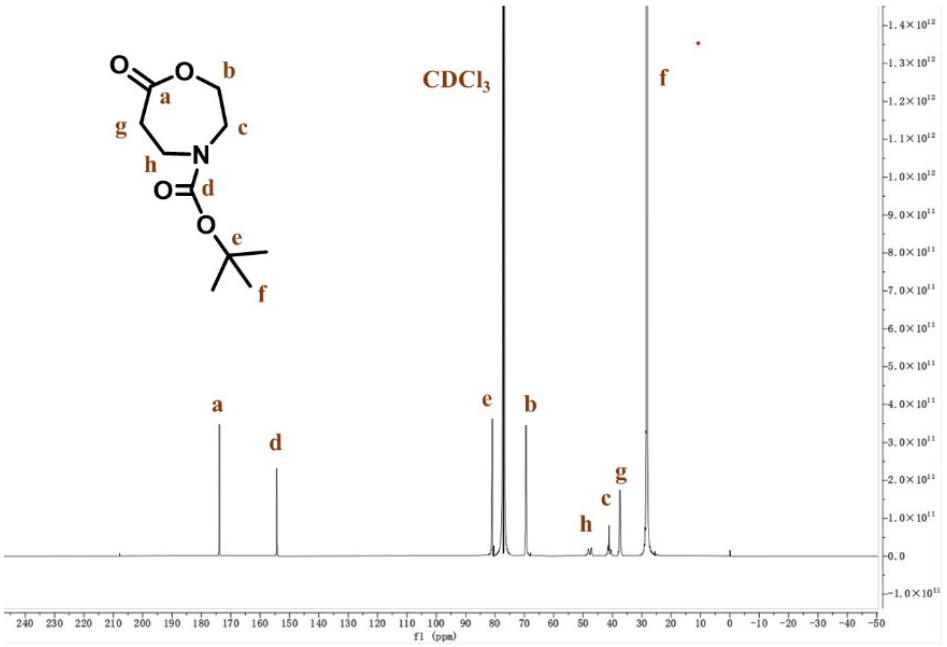

Fig. S15. ^{13}C NMR spectrum of NIPIL

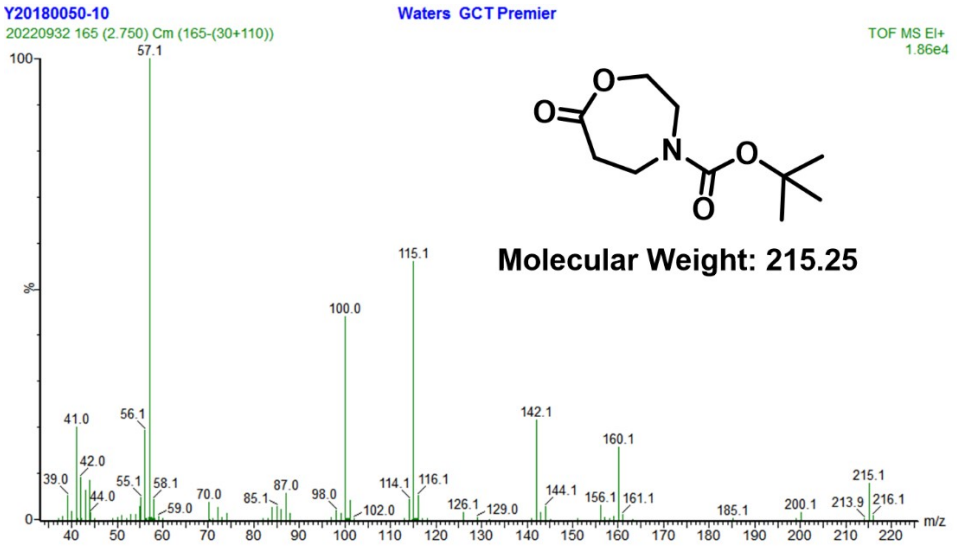

Fig. S16. Electron impact high resolution time-of-flight mass spectrometer of NIPIL

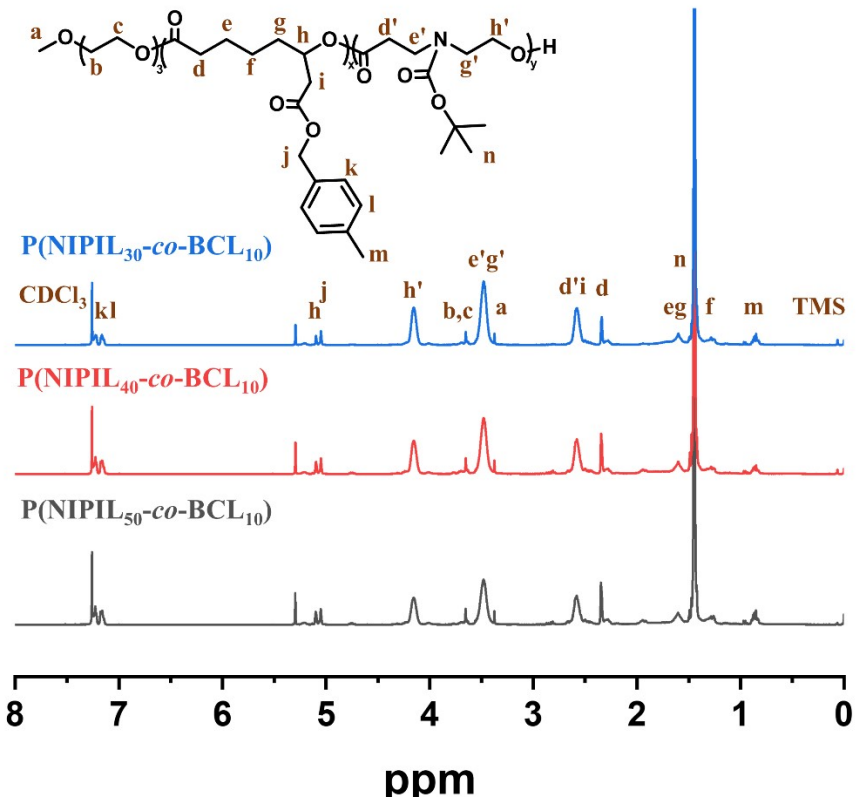

Fig. S17. ^{1}H NMR spectra of P(NIPIL-*co*-BCL)

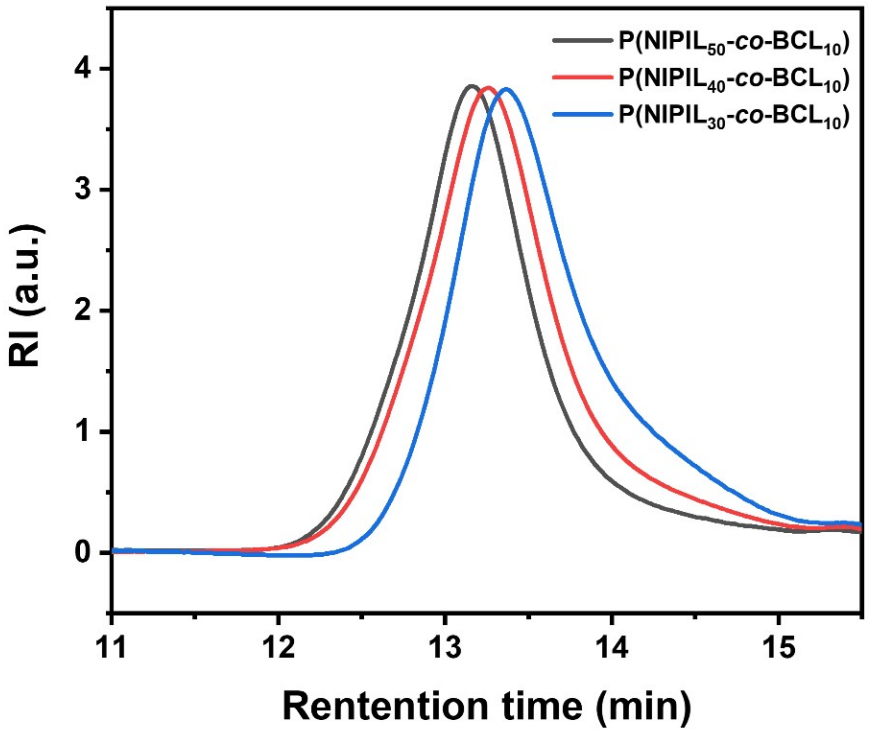

Fig. S18. GPC curves of P(NIPIL-*co*-BCL).

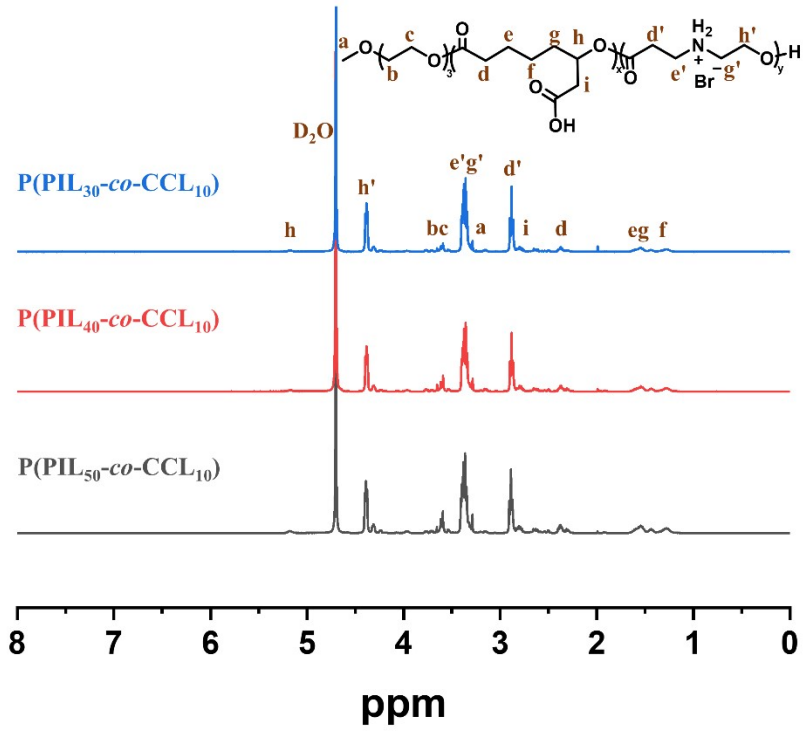

Fig. S19. ^{1}H NMR spectra of P(PIL-*co*-CCL).

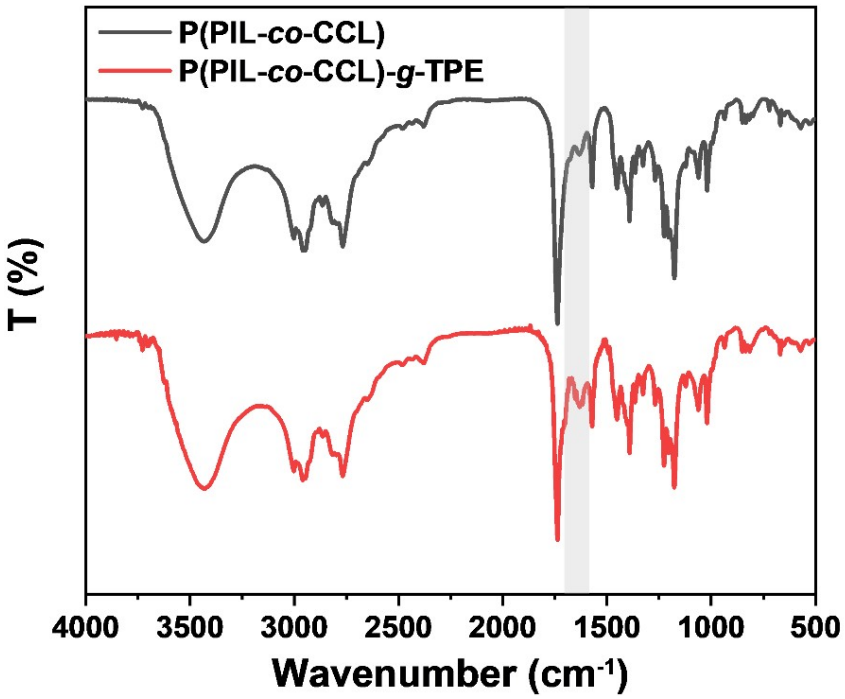

Fig. S20. FT-IR spectra of P(PIL$_{40}$-*co*-CCL$_{10}$) and P(PIL$_{40}$-*co*-CCL$_{10}$)-*g*-TPE.

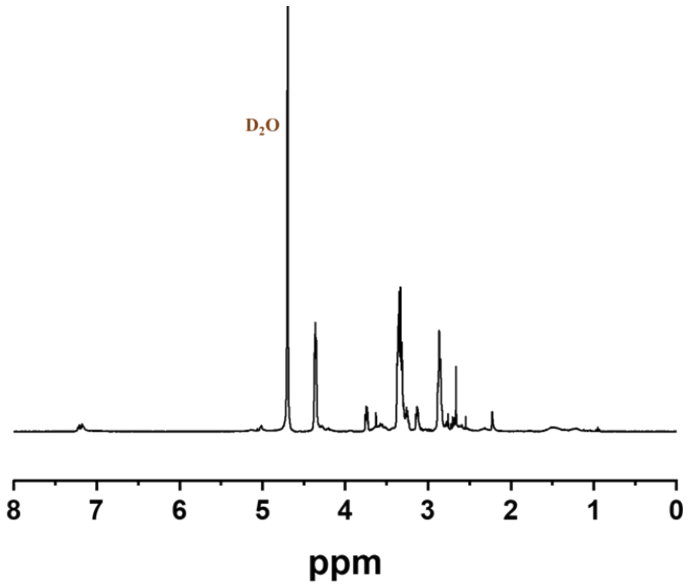

Fig. S21. ^{1}H NMR spectrum of fluorescent polymer (P2) in D_2O.

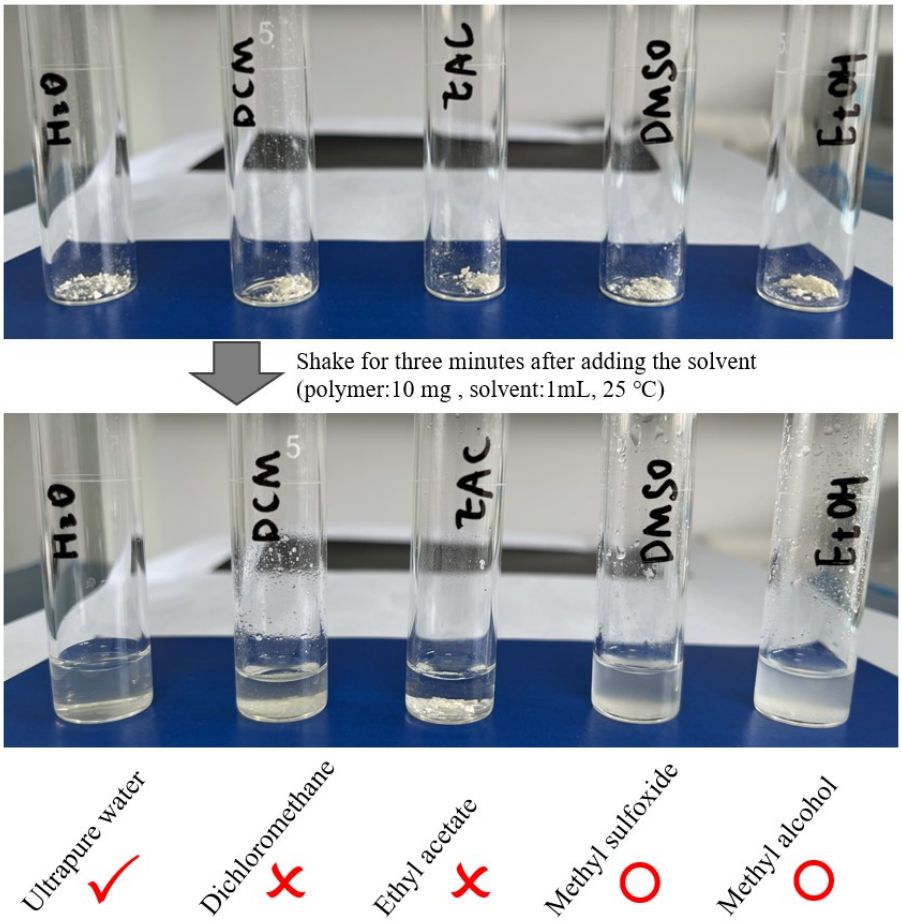

Fig. S22. Solubility of fluorescent polymer (P2) in different solvents

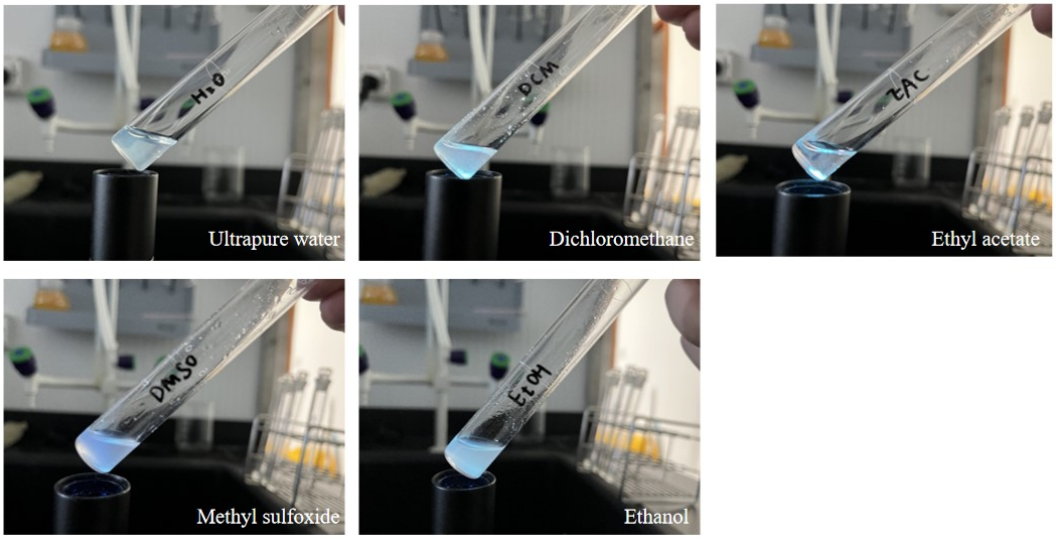

Fig. S23. The luminescence of fluorescent polymer P2 in different solvents (the light source is a 365nm flashlight)

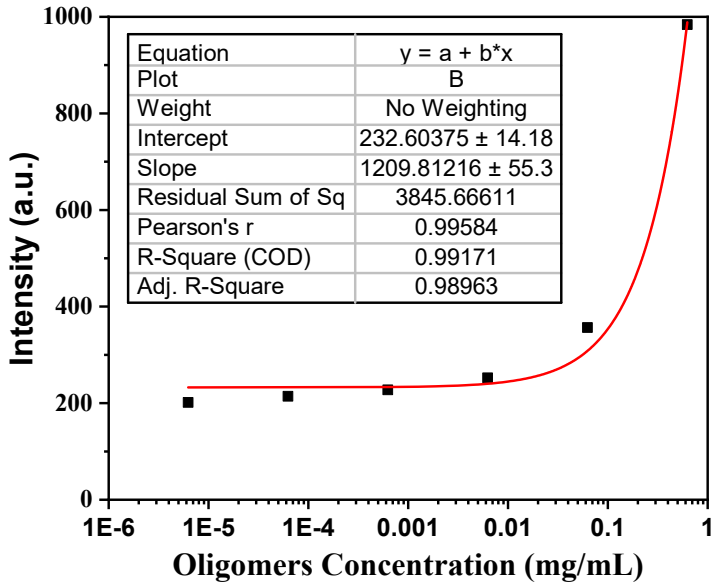

Fig. S24. The relationship between fluorescence intensity and oligomers concentration

1. J. Zhang, Y. Xiao, H. Xu, C. Zhou and M. Lang, *Polymer Chemistry*, 2016, **7**, 4630-4637.
2. J. Zhang, Y. Xiao, X. Luo, L. Wen, A. Heise and M. Lang, *Polymer Chemistry*, 2017, **8**, 3261-3270.
3. C. Fan, Z. Q. Chen, C. Li, Y. L. Wang, Q. Yu and M. Q. Zhu, *ACS Appl. Mater Interfaces*, 2021, **13**, 19625-19632.